Composites: Part A 163 (2022) 107241

Contents lists available at ScienceDirect

Composites Part A

journal homepage: www.elsevier.com/locate/compositesa

Improving the delamination bridging performance of Z-pins through the use of a ductile matrix

E. Santana de Vega *, G. Allegri, B. Zhang, I. Hamerton, S.R. Hallett

Bristol Composites Institute, Queen's Building, University of Bristol, University Walk, Bristol BS8 1TR, UK

ARTICLE INFO

Keywords:
A. Polymer-matrix composites (PMCs)
B. Delamination
E. Pultrusion
Z-pins

ABSTRACT

This paper presents a characterisation of the effect of varying the polymer matrix in Z-pin through-thickness reinforcement in pre-preg based laminates. Four matrix systems of increasing elongation at break are considered, namely: 1) a low glass-transition temperature (LTG) epoxy; 2) a high glass-transition temperature (HTG) epoxy; 3) a bismaleimide triazine (BT); 4) a bismaleimide (BMI). The last matrix is that used in commercially available Z-pins. The manufacturing of T300 carbon-fibre Z-pins employing the first three matrices *via* micro-pultrusion is discussed. The BT resin is considered as a benchmark for the manufacturing process. A preliminary screening of the mode II bridging performance of through-thickness reinforcement manufactured using the three matrix systems is carried out. A novel experimental set-up based on an acrylic glass carrier, which allows the failure mode of the through-thickness reinforcement to be visualised, is introduced. The preliminary tests reveal a 7-fold increase of work-to-failure for the candidates with the highest elongation at break, LTG Z-pins, compared to their baseline BMI-based counterparts. LTG Z-pins were then inserted in quasi-isotropic E-glass epoxy laminates and their bridging performance characterised across the full mode-mixity range. The experimental results indicate that LTG Z-pins provide a peak mode I interlaminar fracture toughness of the order of 40 kJ/m^2, compared to the 28 kJ/m^2 yielded by BMI Z-pins. Moreover, the transition from full pull-out to rupture for the LTG pins occurs at a mode-mixity of 0.55, whereas BMI Z-pins start failing at a mode-mixity of 0.2. The superior bridging performance of the LTG Z-pins is correlated with the enhanced ductility and toughness of the constituent matrix *via* detailed fractographic observations.

1. Introduction

Through-thickness reinforcement is an important means for enhancing the interlaminar fracture behaviour in composite laminates. Several strategies for embedding through-thickness reinforcement in laminates have been proposed in literature. These include 3D fibre textile preforms made through weaving and braiding [1], as well as the introduction of fibres or tows in the Z-direction (*i.e.* through the thickness), using techniques such as Z-pinning/stitching/embroidery [2] and tufting [3]. In most cases, the through-thickness reinforcing component is introduced into dry preforms, prior to the addition of any matrix or matrix precursors. On the other hand, Z-pinning is the most widely employed through-thickness reinforcement technique that is suitable for pre-preg based laminates and consists of the orthogonal insertion of stiff small-diameter rods into ply stacks prior to curing [4]. Z-pins act as micro-fasteners, restraining the opening and sliding displacements of adjacent plies and hence inhibiting interlaminar crack growth [6].

Research work on Z-pinning has been conducted for decades, as evidenced by the extensive reviews available on the subject [5–7]. Key experimental studies have explored the delamination toughening effect of Z-pins in mode I, mode II and mixed-mode loading in quasi-static tests [4,8–10], as well as under cyclic [11–14] and dynamic [15,16] loading. Z-pins can be made of a variety of materials, including metals such as titanium and steel, and fibrous composites. Metallic Z-pins have been shown to provide notable delamination toughening in mode II bridging conditions, yet perform poorly in mode I [4–6,17–19] Attempts to improving the mode I bridging performance of metallic pins include introducing an insertion angle [19] and using "shaped" Z-pins [18].

Although other material combinations are possible [5,6], most studies on composite Z-pins have focussed almost exclusively on T300 unidirectional carbon fibre tows within a bismaleimide matrix (T300/BMI); these pins excel in mode I bridging [4,8,9]. However, the effectiveness of the carbon-fibre/BMI composite Z-pins in preventing mode II delamination is fairly modest [4,9,10,20]. Under mode I loading, the Z-

* Corresponding author.
E-mail address: lm18529@bristol.ac.uk (E. Santana de Vega).

https://doi.org/10.1016/j.compositesa.2022.107241
Received 9 June 2022; Received in revised form 26 September 2022; Accepted 1 October 2022
Available online 7 October 2022

pins will first de-bond from the laminate, and then they will be progressively pulled out against an opposing frictional force [4,21]. Most of the mechanical energy dissipated is associated with the aforementioned pull-out frictional force, which governs the effective toughness enhancement. As the ratio of mode II to mode I increases, the response of composite pins will typically transition from complete pull-out to rupture [9]. The inherent brittleness of BMI composite Z-pins, due to the high crosslink density of the matrix, leads to an onset of rupture at mode-mixity angles above 15-30°. This dramatically reduces the z-pins' interlaminar toughening capability [10] when the delamination has a mode II displacement component.

The loss of performance of composite Z-pins at high mode mixity angles is the key issue addressed in this study. The effect of employing a different matrix system to manufacture composite Z-pins with increased ductility has been explored. First, the manufacturing process for Z-pins, using several alternative resin systems is presented and then a novel method for screening performance in mode II, which entails embedding the Z-pins into acrylic blocks, is discussed. The latter allows the most promising material combinations for manufacturing Z-pins to be identified, which are then tested in composite laminates considering the full range of mode-mixity values, *i.e.* from pure mode I to pure mode II. The objective here is to identify the trend of the apparent fracture toughness provided by Z-pins manufactured with different resin systems, focussing on the transition from complete pull-out to rupture of the through-thickness reinforcement rods.

2. Materials and methods

2.1. Materials

Epoxy resins and hardeners were all supplied by Huntsman Corporation and were used as received. These were: Araldite©LY556, Hardener XB3473, Araldite©LY3508, and Aradur©22962. Bismaleimide and cyanate ester monomers were supplied by Evonik industries (Hannau-Wolfgang, Germany) and Lonza AG (Visp, Switzerland) respectively. Further remarks on the properties of these resins will follow in *Sec*. 2.2. A 1 k tow of T300 carbon fibres was used. Poly(methyl methacrylate) was purchased from RS components UK. BMI matrix Z-pins with T300 carbon fibre were supplied by DPP B.V. Iron (Fe, 99.5%) wires of 0.3 mm diameter were supplied by Goodfellow Cambridge Ltd.

2.2. Resin formulations

Three thermosetting resins were selected to encompass a representative spread of ductility and toughness properties. Hence, selecting a resin specifically designed for increased elongation at break compared to typical BMIs was essential. In conjunction, a resin with properties that are comparable to that of the commonly used BMIs, as well as an intermediate candidate, were also included. Each resin was employed to manufacture z-pins through pultrusion (Section 2.3). The temperature at which this pultrusion took place was optimised for each resin system to promote gelling at a 1 mm/s pulling rate, without affecting the final architecture and consolidation quality of the pin. The three preliminary candidate resins were the following (their physical and mechanical properties are given in Table 1):

- Araldite©LY3508 + Aradur©22962 [22] - Low Tg epoxy (LTG); this is a toughened epoxy resin with considerably large elongation at break. It is characterised by a relatively low Tg as a result. Its components were blended manually at room temperature with a wooden spatula and pultruded (see Section 2.3) at 100 °C, followed by a 2 h cure at 150 °C. The ratio by weight was epoxy (100): hardener (22).
- Bismaleimide triazine (BT): A novel in-house resin blend with comparable mechanical and thermal properties to typical BMIs, but with solvent-free, liquid processing. Its chemistry combines that of cyanate esters and BMIs, enhancing its low temperature processability, ideal as a control candidate. It was pultruded at 200 °C followed by a two stage cure of 4 h at 200 °C and 1 h at 260 °C.
- Araldite©LY556 + HardenerXB3473 [23] - High T_g epoxy (HTG): An epoxy resin with a moderate elongation at break, higher than the BT and lower than the LTG, albeit with increased temperature stability. Its components were manually blended at room temperature with a wooden spatula and pultruded at 180 °C, followed by an hour cure at the same temperature. The suggested ratio by weight was epoxy (100): hardener (23).

2.3. Fabrication of Z-pin stock

The Z-pin candidates were manufactured by micro-pultrusion. The steps involved in the manufacturing process can be summarised as follows:

1. The carbon fibre tow was unwound from the bobbin and fed through a 1 mm diameter guide hole and across a set of rollers. The fibre tow was then impregnated in a resin bath, which contained the appropriate resin blend.
2. The impregnated tow was then fed into a pre-heated die which shaped and gelled the resin. The temperature to which the die was heated varied depending on the resin (see Section 2.2). These die temperatures were the result of multiple manufacturing trials, through which the pultrusion process for each candidate matrix was optimised. The die itself was assembled in two steel parts, with a 0.3 mm diameter hole along its 130 mm length.
3. The tow was pulled for a total of 60 cm per batch at a pulling rate 1 mm/s. The gelled composite rod remained under tension during the pultrusion process. The partially cured rod was carefully cut and placed inside an oven to undergo a complete curing cycle. To ensure that the shape of the rod-stock was maintained, a light weight was hung from one of its ends as it cured.

Fig. 1 shows the final microscopy of the Z-pins after optimising the pultrusion process for each matrix type. The quality of the manufactured pins is comparable to that of the DPP produced carbon-fibre/BMI pins (Fig. 1A), specifically in terms of void content and fibre volume fraction. It is worth mentioning that the geometrical stability of the cross-section was slightly inferior to that of BMI pins. Although the average diameter was consistent, it was not as circular shaped. The nominal diameter was taken to be that of the pultrusion die, 0.3 mm. Nevertheless, the impact of this irregular cross-section was expected to be minimal and apparent in the scatter of the results.

Table 1
Typical properties of the resin systems used in this study. [a]The mechanical properties of the BT resin are expected to lie within the boundaries of its constituent resin systems, hence that of cyanate esters and bismaleimides have been quoted [24].

Resin	Processing viscosity	Pot life	Gel Time (Temp)	Tg	Elongation at break	Flexural Modulus	Ultimate Strength
Unit	*mPa.s*	*h*	*min(°C)*	*°C*	*%*	*GPa*	*MPa*
BT [24,25]	208	Several days	–	226–235	2.5–2.8 (CE)[a]	2.7–5.9 (CE)[a]	56–120 (CE)[a]
					1.6–2.3 (BMI) [a]	3.6–4.8 (BMI)[a]	55–90 (BMI) [a]
HTG [23]	5200–6000	32–37	9–13 (180)	185–194	5.5–6.5	2.7–2.9	110–120
LTG[22]	1800–2100	1–2	4–8 (120)	144–154	8–10	2.7–2.9	120–135

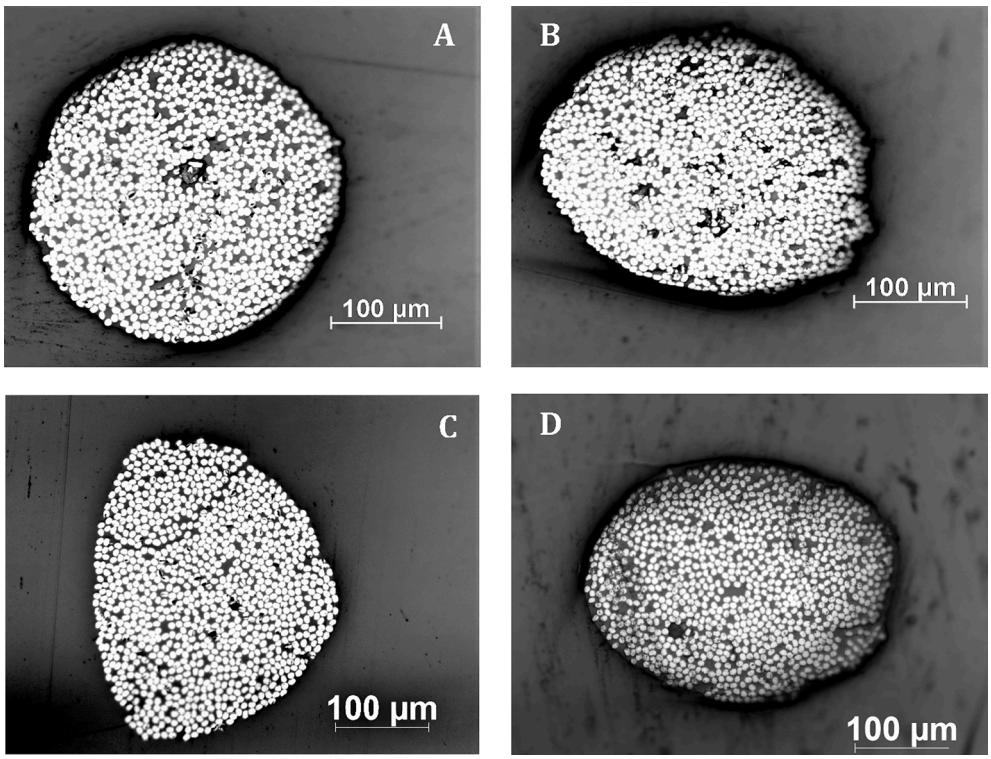

Fig. 1. Optical micrographs showing the as-manufactured cross-sectional microstructure of the (A) BMI, (B) LTG, (C) HTG and (D) BT carbon-fibre composite Z-pins.

2.4. Fabrication of test coupons

Two sets of test coupons were prepared. The aim of the first set was to characterise and visualise the behaviour of the three new types of pins when inserted into an acrylic glass coupon and loaded under pure shear, *i.e.* in mode II. The second set of coupons were manufactured by inserting the most promising Z-pin candidate configuration in a composite laminate.

2.4.1. Acrylic glass substrate coupons

Acrylic-substrate coupons were manufactured by laser-cutting a 4 mm thick acrylic sheet into 16 mm × 16 mm blocks. A 0.35 mm hole was subsequently machined at the geometrical centres of the individual blocks. The Z-pins were then inserted through two blocks that had been brought together in contact. Each block mimicked the laminate stack present at either side of a delamination. A single drop of ethyl-2-cyanoacrylate adhesive was used to bond the ends of each Z-pin to the acrylic block. This was done to avoid the sliding and rotating of the pin inside of the coupon, as there was a 0.05 mm clearance between the pin and the hole.

The main reason for considering this coupon configuration was to perform a rapid evaluation of the mode II (shear-loading) response of each pin type prior to manufacturing actual Z-pinned laminate coupons. Additionally, the proposed set-up allows the mechanical response of the pin during the test procedure to be visualised, while having a foundation stiffness comparable to that provided by a quasi-isotropic laminate. Hence, this method was ideal for an efficient performance comparison among the different pin compositions. As mentioned before, the best performing pin was then used in laminate coupon tests.

2.4.2. Composite coupons

Composite coupons comprising unidirectional E-glass fibres in a Hexcel 913 epoxy were manufactured by hand-lamination of prepreg. This resin can be cured at a relatively low temperature of 125 °C, and this ensures that the T_g of the LTG pins (140 °C) is never reached. The stacking sequence employed was [(0/45/90/-45)3 /0]s //[(90/-45/0/45)3/90]s, with a PTFE release film at its midplane indicated by '//'. This stacking sequence results in symmetric and balanced top and bottom halves. It is anti-symmetric overall, which results in a 0/90 midplane to reduce the fibre nestling effect, which would otherwise increase interlaminar friction at the delamination plane.

The final geometry of the coupons is almost identical to that of the acrylic blocks with dimensions of 16 mm × 16 mm × 8 mm. To manufacture the specimens, a 150 mm × 150 mm laminate was initially laid up, with a square array of Z-pins inserted manually at 22 mm intervals in the un-cured laminate. The Z-pinned laminate was then cured in an autoclave, following the material supplier's guidelines. The final step of the specimen preparation was to machine the laminate into individual coupons, by means of a water-cooled diamond disk cutter. Fig. 2 shows a schematic representation of a single coupon.

Once the coupons had been manufactured, the microstructural

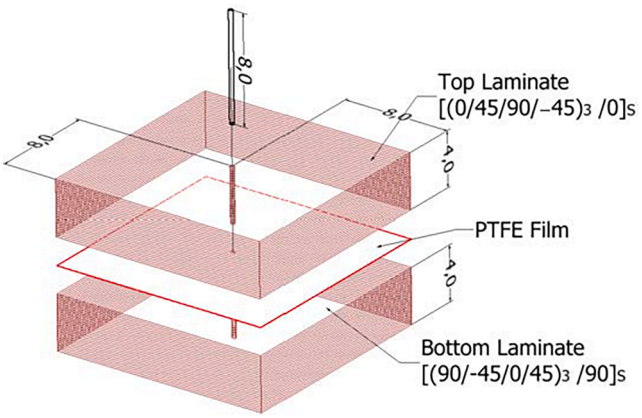

Fig. 2. Schematic representation of the test coupons used in the single pin laminate tests. Note the PTFE is used as a means of creating a delamination plane. (For interpretation of the references to colour in this figure legend, the reader is referred to the web version of this article.)

architecture in the neighbourhood of individual Z-pins was evaluated through optical microscopy. Fig. 3 and Fig. 4 show the cross-sectional and transverse cut-outs respectively of the Z-pins embedded in the laminate. The Z-pin/laminate interface may be damaged, due to the mismatch between the thermal expansion coefficients of the pin and the laminate [26,27], but there is no evidence of cracks at the said interface in Fig. 4. Moreover, no cracks were observed within the Z-pins prior to the application of mechanical loading. This microscopic characterisation is helpful in explaining some of the results from the mechanical tests that follow. It must be noted that there are some voids present in the substrate laminate. However, as the bridging tests rely on an already fully developed delamination plane and the laminate itself will only carry a minimal load, these voids have no effect on the experimental results. Note that a resin pocket was present around the pin, caused by the displacement of the laminate fibres during Z-pin insertion. This is a widely documented feature of Z-pinned laminates [6].

2.5. Mechanical characterisation procedure

A modified Arcan rig (Fig. 5) was used to test the coupons under mixed-mode loading [10]. The coupon can be rotated at 15° intervals from pure mode I (0°) to pure mode II (90°). The rig was mounted on an Instron 8852 servo hydraulic machine. It was set-up in such way that each half of the coupon moved in opposite directions along the vertical axis. A test rate of 1 mm of vertical displacement per minute was used for all samples. All the coupons were brought to failure (full pin pull-out from one side or pin rupture). The acrylic coupons were tested only under mode II loading conditions, from which enough energy dissipation data could be obtained to compare their performance. The best performing candidate was then tested through a representative range of the full mode-mixity, together with the BMI resin pins for benchmarking. A minimum of four successful tests were carried out at each angle.

3. Results and discussion

3.1. Acrylic substrate coupons: Preliminary characterisation

The key findings of the initial characterisation study carried out on the three new pin types by using acrylic blocks are summarised in Fig. 6. Additionally, the BMI-based pins as well as some iron (Fe, 99.5%) pins with a 0.3 mm diameter and the relevant data are included in the graphics.

The work to failure chart shows that the LTG pins exhibited the largest energy absorption prior to failure among the three newly manufactured candidates. The energy required to bring the LTG pins to complete failure was 400% higher than that of the BMI pins; the latter was similar to that of the control candidate (BT), as expected given the similar matrix composition. Consistent with previous reports [4,19], the steel pins out-performed all composite candidates in mode II. However, the LTG pins showed a behaviour similar to that of these metallic pins, with a load sustained throughout a large shear displacement range. This is reflected in the large energy values observed in Fig. 6. This suggests that the LTG pin did not fail after the peak load and was instead able to deform plastically under a transverse load. Hence, despite the tests having been carried out in mode II, the pins were fully pulled out because of the axial force that resulted from the large cross-sectional rotations. It is worth stressing that complete pull-out is commonly observed in composite Z-pins only in mode I dominated loading, and it represents the main energy-absorbing mechanism [6,21,28,29]. On the other hand, complete pull out may occur in metallic Z-pins under mode II loading [4], but it has never been observed in composite pins before. The ability of the LTG pins to attain large inelastic deformations can be clearly appreciated in the mid-test images shown on the left image of Fig. 7. On the other hand, the images on the right-hand side of Fig. 7 show the small amount of lateral deformation that the BMI Z-pins can support, which is associated with early failure and no pull out.

These preliminary results do not represent the pure mode II behaviour of the pins within a composite laminate, yet they highlight the potential of the LTG pin to provide an increased delamination toughness under high mode II loads. As a result, the LTG pin was selected as the candidate for the characterisation of the bridging response in a cured composite laminate across a full range of mode mixites.

3.2. Single pin delamination bridging tests

The superior transverse mechanical performance of the LTG pins was observed in the acrylic coupon tests, hence the next logical step was to evaluate how this translates to their delamination bridging behaviour within a cured composite laminate. This section summarises the results of single-pin bridging tests carried out throughout a full range of load mode-mixity angles for both the LTG pins and their commonly used counterparts (BMI pins).

3.2.1. Apparent fracture toughness and pin misalignment calculations

The measure of energy absorption obtained in these tests is expressed as apparent fracture toughness (G*). The latter corresponds to the energy dissipated through crack bridging per unit delamination area [20]. This is calculated from the energy absorbed to failure by a single Z-pin ($\Psi(\phi)$) and the pining areal density ρ *via* the following relationship [20]:

$$G^{*}(\phi) = \frac{4\rho}{\pi D^{2}}\Psi(\phi) \tag{1}$$

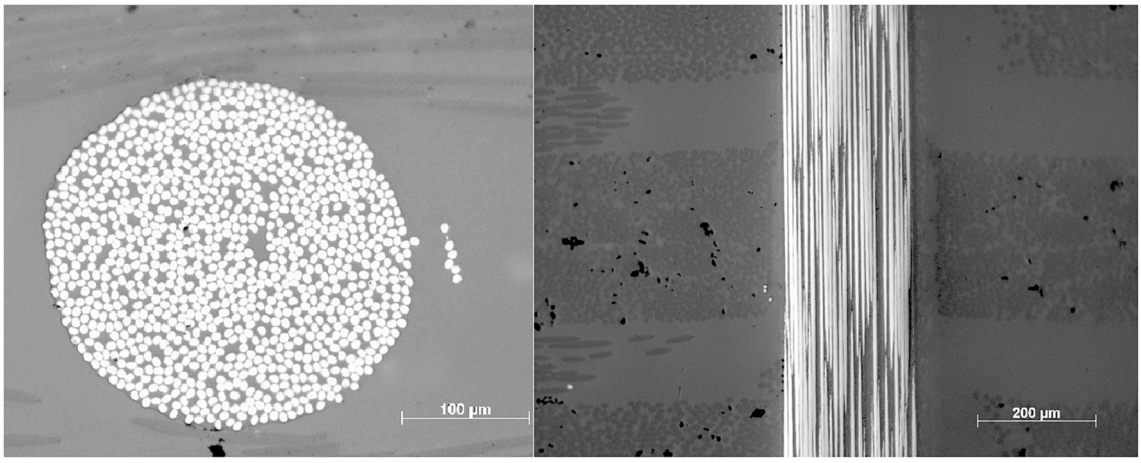

Fig. 3. Micrographs showing the microstructural features of BMI pins within a E-glass/epoxy laminate after the insertion and curing stages.

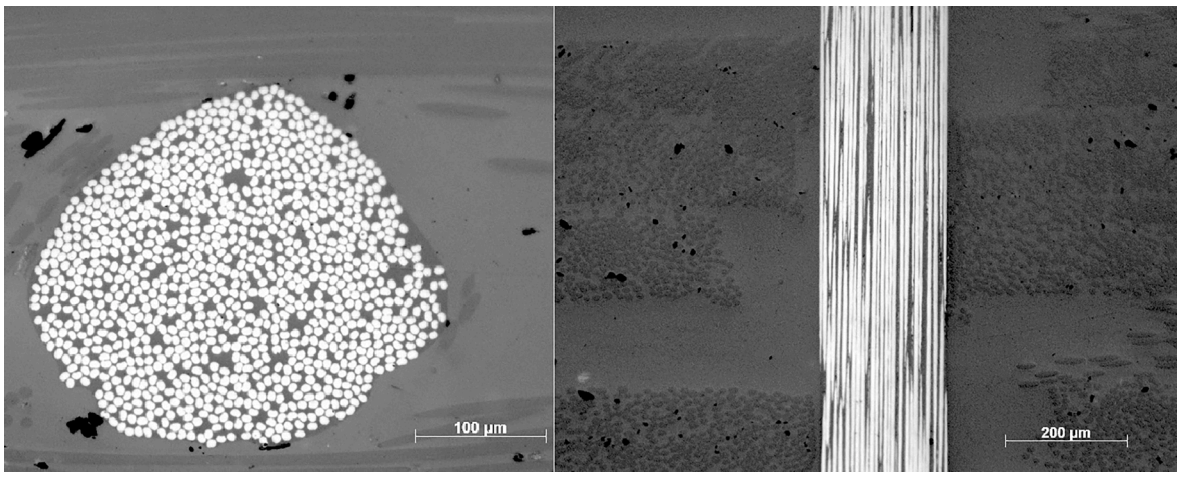

Fig. 4. Micrographs showing the microstructural features of LTG pins within a E-glass/epoxy laminate after the insertion and curing stages.

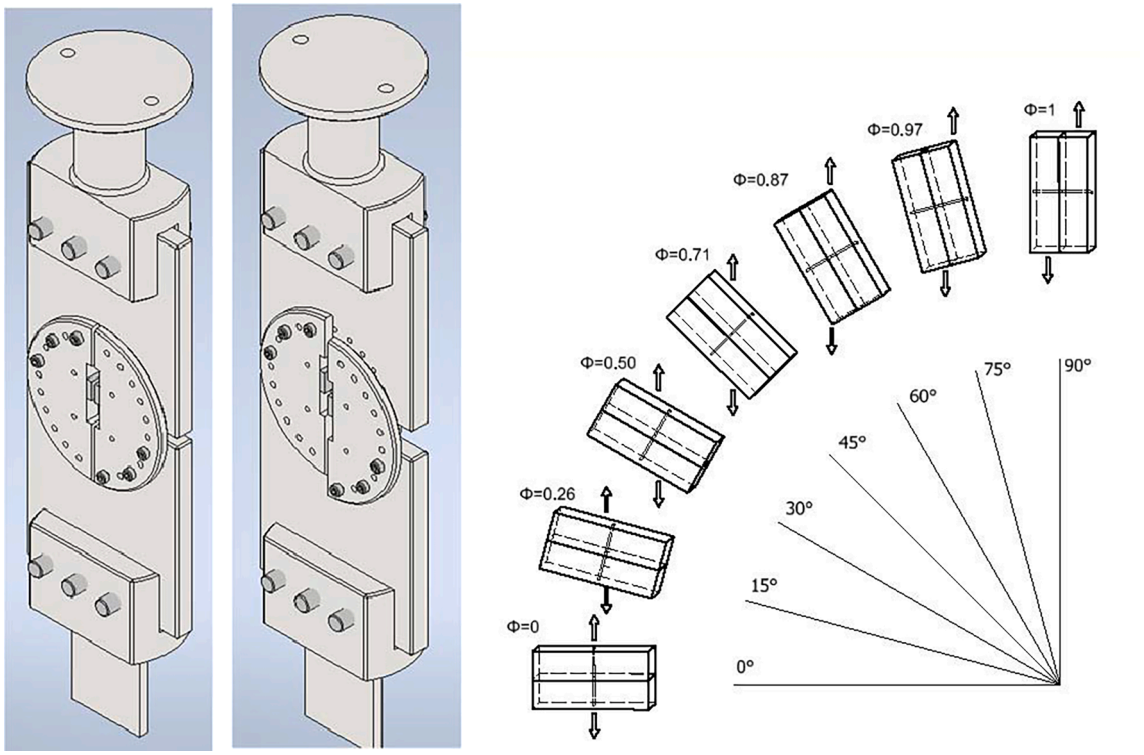

Fig. 5. CAD representation of the Arcan rig fixture and its operation. The diagram on the right represents the different configurations possible and their respective mode-mixity ratios.

where D is the diameter of a single pin; $\Psi(\phi)$ is calculated from the area under the load–displacement curves, and ρ is given by:

$$\rho = \frac{\pi D^2}{4W^2} \tag{2}$$

where W is the unit cell edge length associated with a single Z-pin. For this study, we assume an areal density of 0.02.

The actual mode-mixity to which each pin is subjected is determined by direction of the total load with respect to the pin axis. The Arcan rig (Fig. 5) allows the user to rotate the coupons by 15° increments and achieve nominal mode mixity values. However, the manufacturing process of the Z-pinned laminates, including pin insertion and consolidation results in minor misalignment of the pins with respect to the laminate's through-thickness axis. As a result, the true load mode mixity will differ slightly from the nominal mode mixity. To account for the pin misalignment, the deviation of each individual Z-pin in the × and y directions was measured and considered in the actual mode-mixity (ϕ) calculation using Equation 3. This method of accounting for pin misalignment was previously introduced by researchers at Bristol Composites Institute [10,20,26]. The pin misalignment and conventions used are represented schematically in Fig. 8. The actual mode mixity is given by:

$$\phi = \sqrt{cos^2\chi sin^2\zeta + sin^2\chi(sin^2\psi + cos^2\psi cos^2\zeta) - \frac{1}{2}sin2\chi sin2\zeta cos\psi} \tag{3}$$

In Equation (3), χ is the angle between the normal loading direction and pin insertion axis (*i.e.* the angle of rotation of the coupon). The relative offset angles ζ and ψ correspond to the misalginements of the

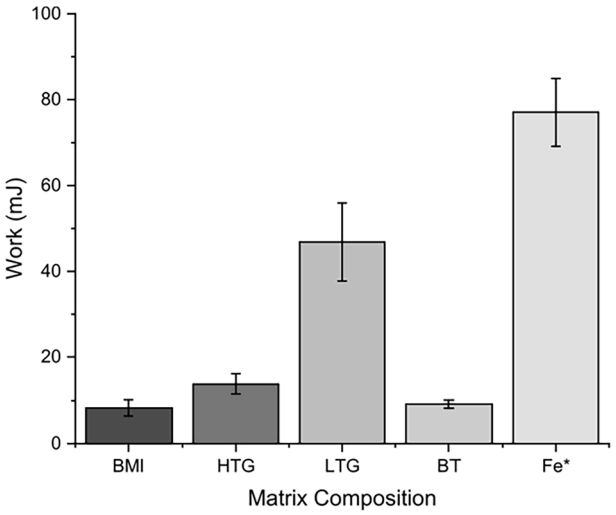

Fig. 6. Average work carried out by each Z-pin type in an acrylic coupon prior to failure. *Pins made out of pure (99.5%) iron wire for a direct comparison with metallic ductility.

pin from the z- and x-axis respectively, and these can be calculated from the misalignment angles α_{13} and α_{23} (see Fig. 8) using Equations 4 and 5:

$$tan\zeta = \sqrt{tan^2\alpha_{13} + tan^2\alpha_{23}} \tag{4}$$

$$tan\psi = \frac{tan^2\alpha_{23}}{tan^2\alpha_{13}} \tag{5}$$

3.2.2. Summary of mixed-mode results

The apparent toughness values attained by both the BMI and the LTG Z-pins are plotted in Fig. 9. Note that every pin tested has been considered individually, as each Z-pin was subjected to different load mode-mixities due to misalignment. In the aforementioned plots, there are three key regions that must be carefully examined: 1) mode-mixity values close to mode I ($\phi \approx 0$); 2) close to mode II ($\phi \approx 1$); and 3), the region that corresponds to a 0.2–0.6 mode mixity.

Firstly, throughout the full mode-mixity range, the LTG pins exhibited a higher apparent fracture toughness on average compared to the BMI-based ones. For a nominal mode II load, there is arguably no statistically significant difference between the responses of the LTG and the BMI pins. This is a consequence of the fact that the mode II fracture toughness of Z-pinned laminates is controlled by the fracture toughness for tensile fibre failure of the pins [26], and both the configurations considered here (*i.e.* LTG and BMI) were manufactured using T300 fibre as the reinforcement. The total energy ranges from 4 to 7 mJ at a mode mixity of 0.9–1. As the load mode-mixity ratio decreases and the amount of crack opening increases, the difference between the LTG and the BMI pins gradually increases, being on average almost 5 kJ/m^2 higher at a mode mixity of 0.7.

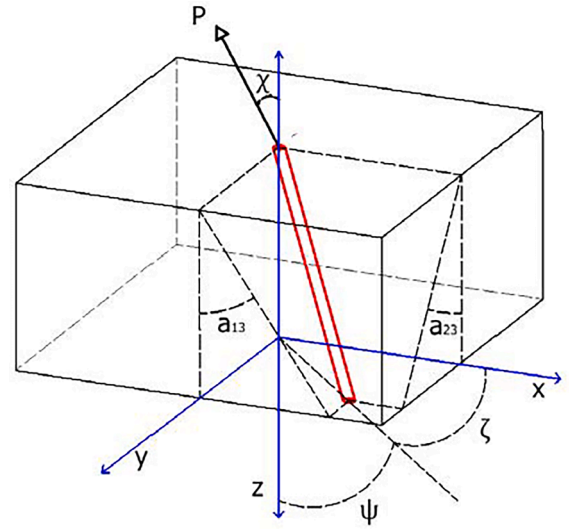

Fig. 8. Diagram illustrating pin misalignment and the conventions used to calculate the true mode-mixity with respect to the loading direction. (For interpretation of the references to colour in this figure legend, the reader is referred to the web version of this article.)

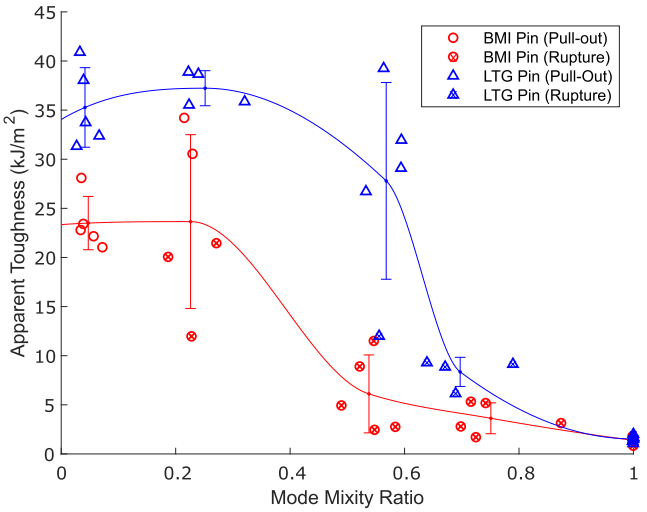

Fig. 9. Apparent delamination toughness of the BMI and LTG pins throughout the full load mode-mixity range, normalised for an aerial density of 0.2%. Note that in the shaded regions, the lower energy pins have typically ruptured, whilst the higher energy ones have been pulled out. (For interpretation of the references to colour in this figure legend, the reader is referred to the web version of this article.)

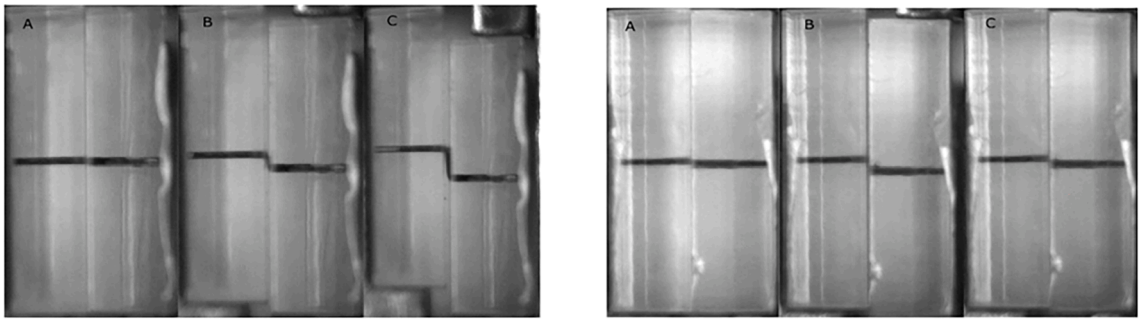

Fig. 7. Mid-test chronological images of the LTG (left) and BMI (right) composite pins when transversely loaded within an acrylic substrate.

The largest difference between the LTG and BMI pins occurs at a mode-mixity ratio of 0.5–0.6. Here, stable pull-out of the LTG pins is possible, while rupture of the BMI pins is consistently observed. Whilst the BMI pins exhibit a maximum toughness of 11.5 kJ/m^2 within this mode-mixity range, the LTG pins can provide toughness values as high as 39 kJ/m^2. This region corresponds to the rupture to pull-out transition for the LTG pins, as is highlighted by the blue shade in Fig. 9 between 0.55 and 0.59 mode ratios. A similar transition region (shaded in red) is observed for the commercial BMI pins, although this occurs in a lower mode-mixity band, *i.e.* between 0.19 and 0.23, hence closer to mode I conditions. The position of this transition for the BMI pins is shifted more closely towards mode I than in the tests presented by Yasaee *et al.* [10]. This could be because of a higher void content of the Z-pins used in [10], as will be discussed subsequently. Lastly, in mode I dominated conditions ($\phi \approx 0$), both pin types consistently exhibit full pull out. Nevertheless, the LTG pins still provide a higher apparent toughness compared to the BMI pins in the full pull-out regime.

Regarding peak bridging forces, the experimental results are affected by a significant amount of scatter. As can be observed in Fig. 10, throughout all five load mode-mixity values characterised, the standard deviation bars for the two types of pins overlap. This suggests that the difference between the peak force results for the two Z-pin types is not statistically significant. The peak force corresponds to the load necessary to either rupture the pin at high mode-mixity values or initiate pull-out for lower ones. In mode II dominated conditions, both pin types exhibit comparable results. On the other hand, the differences observed in pull-out dominated regions depend on the strength of the pin-laminate interface, which are affected by both the chemical compatibility of the matrix systems and the thermal expansion mismatch during post-cure cool down [212627]. Nevertheless, the micrographs in Fig. 3 and Fig. 4 show how there is no visually observable difference of the pin-laminate interphase between the BMI and LTG pins once embedded in the laminate.

Both the shift of the pull-out-to-rupture transition region and the overall increased apparent toughness of the LTG pins can be associated to the superior toughness and ductility of the constituent matrix. The combination of factors that lead to this behaviour will be discussed in further detail with the aid of microscopy in the next sections.

3.2.3. *Pull-out to rupture transition regions (ϕ = 0.20 –0.60)*

Figs. 11 and 12 show the typical load–displacement relationship for the pull-out to rupture transition regions of the BMI pin (ϕ = 0.19 –0.23) and the LTG pin (ϕ = 0.55 –0.59**).** The behaviour of the pins in the transition region is similar for both types, albeit occurring at different mode-mixity ranges. In both cases, the pins that were fully pulled out exhibited a large energy absorption capability, whilst the ruptured pins failed following partial pull-out.

The mechanism by which the LTG pins can be pulled out at a higher mode-mixity ratio can be understood in terms of the ratio of axial to shear stress acting on the pin. As the pin is loaded, both axial and transverse shear stresses develop. At high mode-mixity ratios, the transverse shear dominates, whilst the opposite occurs in mode-I dominated delamination. However, as the pin gradually bends under the load (as could be seen in the preliminary tests in Fig. 7), the initial transverse shear stress transitions into axial stress, because of the rotation of the Z-pin cross section. Both pin types comprise longitudinal carbon fibres, which can sustain large axial stresses. Thus, if enough transverse shear stress is transferred to axial loading before it can cause the transverse rupture of the pin, the pin will reach a stable pull-out condition. The initial magnitude of shear stress that can be transferred into axial stress is directly proportional to the pin's ability to deform and bend, which is affected by the ductility of matrix in a composite Z-pin. At mode-mixity ratios above 0.2, the highly brittle BMI-based pins are not able to reach a stable pull-out stress state without rupturing. On the other hand, the LTG pins are able to accommodate enough bending deformation to allow full pull-out up to a 0.6 mode-mixity.

The ability of the LTG pins to accommodate more bending deformation can be appreciated from their post-failure microscopy images in Fig. 13. In both cases, the pin has been pulled out at a load mode-mixity ratio of around 0.2. The LTG pin has been visibly deformed in a permanent fashion, highlighting its increased ductility and ability to yield. The BMI pin maintains a relatively straight longitudinal axis. In the BMI pin, some cracks have already propagated transversely across the fibres, and these promote the premature failure of the pin. The LTG pin, however, exhibits predominately longitudinal matrix cracking, *i.e.* splitting. These splits, that formed due to the increased bending acting on the pin, made it more compliant, thus delaying or even inhibiting fibre failure and allowing full pin pull-out [26 9 30].

Evidence of an extensive longitudinal shear (splits) is visible in Fig. 14. This shows one of the LTG pins that ruptured in its transition region, with significant fibre fibrillation and a characteristic "brush head" failure. Similar failures have been observed previously in miniature three-point bend tests reported by Allegri *et al.* [20] and in previous

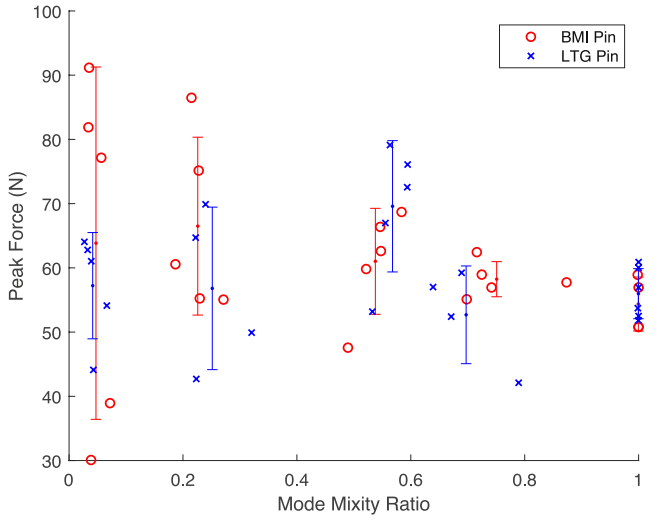

Fig. 10. Peak force exhibited by each Z-pin tested at the different load mode-mixity ratios. Standard deviation bars and means have been plotted to aid in evaluation. (For interpretation of the references to colour in this figure legend, the reader is referred to the web version of this article.)

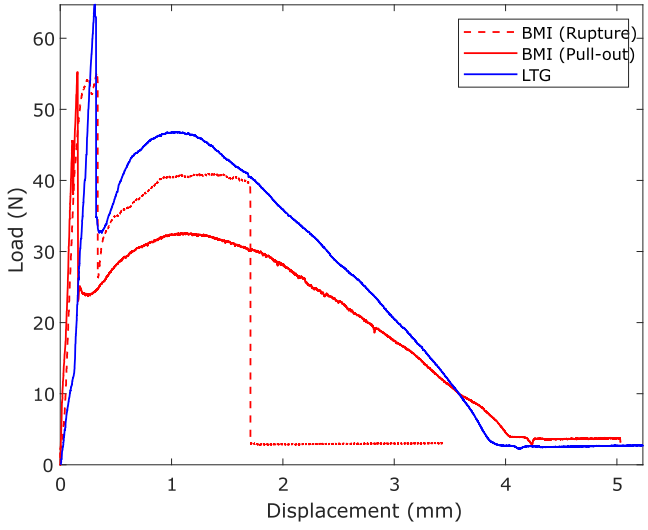

Fig. 11. Representative curves for a load mode-mixity ratio of 0.2. Note this is the transition region for the BMI pins, where all LTG pins were able to fully pull out. (For interpretation of the references to colour in this figure legend, the reader is referred to the web version of this article.)

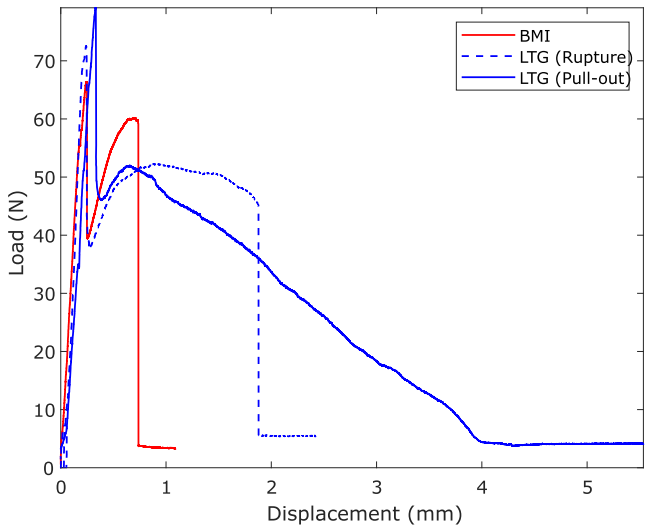

Fig. 12. Representative curves for a load mode-mixity ratio in the region of 0.55. Note this is the transition region for the LTG pins, where all BMI pins ruptured. (For interpretation of the references to colour in this figure legend, the reader is referred to the web version of this article.)

mixed-mode tests carried out by Yasaee *et al.* [10], albeit at lower mode-mixity angles. In comparison, the fracture surfaces of the BMI pins in Fig. 14 exhibit significantly less fibrillation, with clean transverse cracks of brittle nature. Moreover, the cracks follow a significantly more tortuous path through the cross-section of the LTG pins. It is interesting to note that failure occurs at the zones of maximum tensile stress for both the LTG and BMI pins. Fibre failure ultimately occurs at these points, located close to the delamination surfaces at the side that is loaded under tension [9,20].

3.2.4. *Mode I dominated crack bridging ($\phi \leq 0.1$)*

For load mode-mixities closer to mode I, both BMI and LTG pins consistently pull-out. The apparent fracture toughness of the pins in this case mainly results from the frictional force developed during pull-out. It is clear from Fig. 15 that the frictional force required to pull out the BMI pins is typically lower than for the LTG ones. The micrographs in Fig. 16 do not show a notable difference between the two pulled-out pins.

In both cases, a large peak force is initially required to de-bond the pin from the laminate, which is consistent with previous experimental observations [4,10,21]. After the post-debonding drop in force, the BMI pins quickly reach the peak frictional force. In contrast, the LTG pins exhibit a relatively large, gradual increase in the frictional force. This may be also due to local deformations of the more ductile matrix at the pin-laminate interface. As the LTG is pulled out, the toughened epoxy resin may yield locally as it is subjected to the frictional contact. The process would act as an energy absorbing mechanism which will in turn

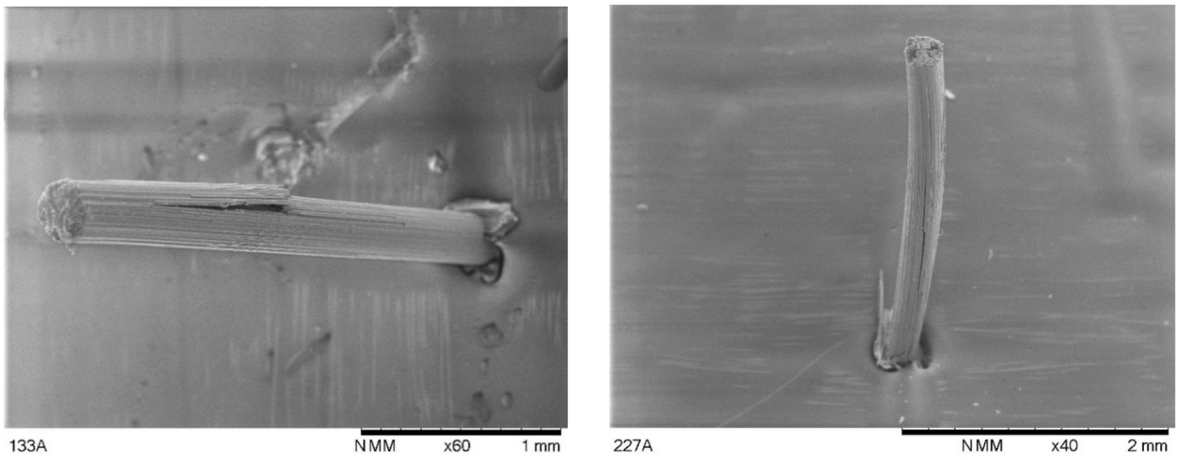

Fig. 13. SEM images of BMI (left) and LTG (right) Z-pins pulled out at load mode-mixity ratio of 0.2.

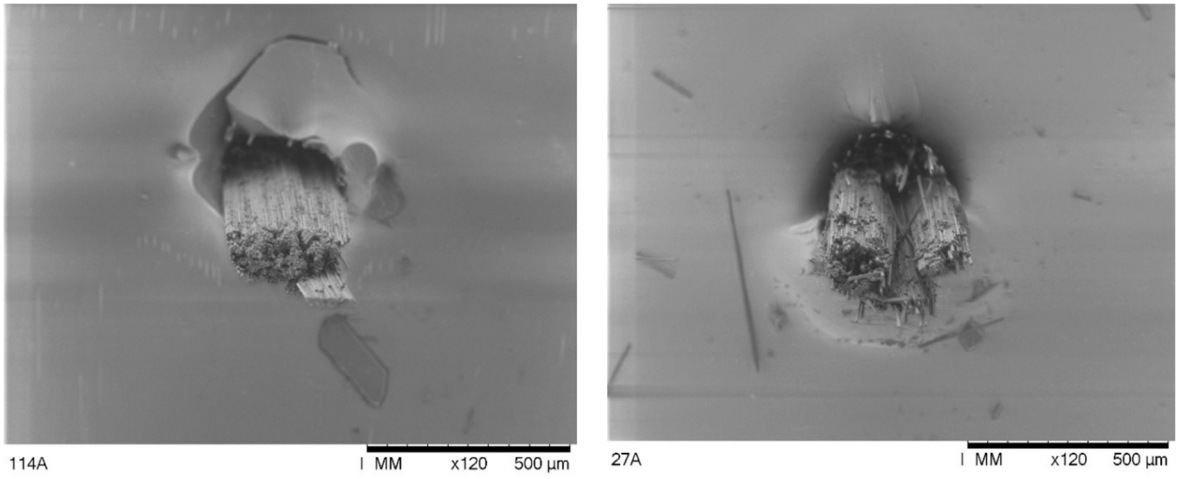

Fig. 14. SEM images of BMI (left) and LTG (right) Z-pins which ruptured at load mode-mixity ratio in the region of 0.5–0.6.

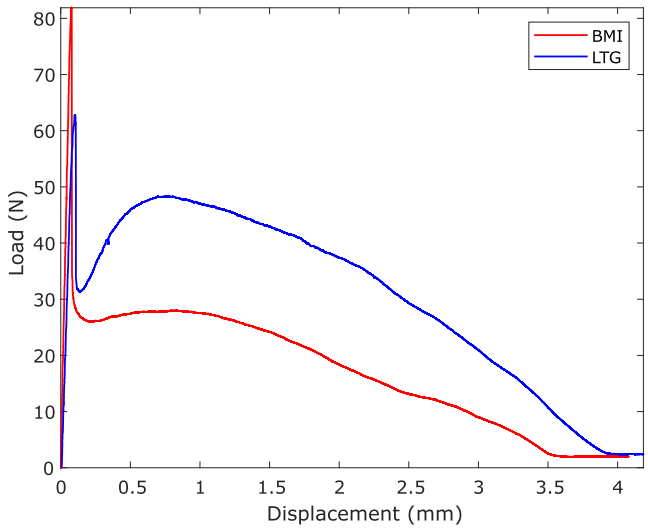

Fig. 15. Representative load–displacement curves for pins pulled out at primarily mode-I load conditions. (For interpretation of the references to colour in this figure legend, the reader is referred to the web version of this article.)

also increase the surface roughness of the pin itself, further increasing the friction between the surfaces. The overall result is a higher apparent toughness exhibited by the LTG pins under mode I dominated loading.

3.2.5. Mode II dominated crack bridging ($\phi \geq 0.6$)

For loading scenarios approaching mode II ($\phi \approx 1$), the difference in energy absorption between the LTG and BMI is small. Both pins fail by transverse rupture, as is evident from the load–displacement curves shown in Fig. 17. This is a result of the high shear stress acting on the pin. The pins are highly constrained within the laminate, which reduces their capability to bend through lateral support. As a result, the bending to shear ratio remains low prior to failure, preventing most of the axial transfer of stress.

At a load mode-mixity ratio of around 0.7, both pin types still rupture. However, the relatively better performance of the LTG pin is again due to its the ability to deform and sustain load through axial stresses rather than shear. Most of the LTG specimens showed an initial debonding and partial pull-out, as is evident from the load–displacement curve in Fig. 17. In the micrograph in Fig. 18, partial pull out of LTG Z-pins is visible, along with some fibre fibrillation and some plastic flow of the matrix. In comparison, the BMI pins exhibit the typical transverse rupture load–displacement curve that has been observed under mode II loading. Microscopy images consistently show a clearly brittle fracture surface, with no visible pull-out. The small residual load observed after pin rupture corresponds to the friction between the tip of failed pin and the surface of one of the sub-laminates at the delamination plane. This is caused by the small but unavoidable compressive force arising between the two parts of the test coupon.

4. Conclusions

From the results of the experimental characterisations presented in this paper, the following conclusions can be drawn:

1. Employing an acrylic glass carrier to study the mode II performance of Z-pins provides a quick and effective method to qualitatively assess the failure behaviour of through thickness reinforcement under transverse load, in particular for screening the "*in-situ*" ductility of through-thickness reinforcement. However, the acrylic-glass carrier cannot fully represent the actual constraint exerted by a laminate on a Z-pin, as the insertion hole must be larger than the Z-pin diameter. Hence, the apparent mode II toughness yielded by tests *via* acrylic glass carriers significantly overestimates the actual performance of through-thickness performance in real laminates.
2. The ductility of the constituent matrix has a strong influence on the bridging performance of Z-pins. More in detail, a ductile matrix

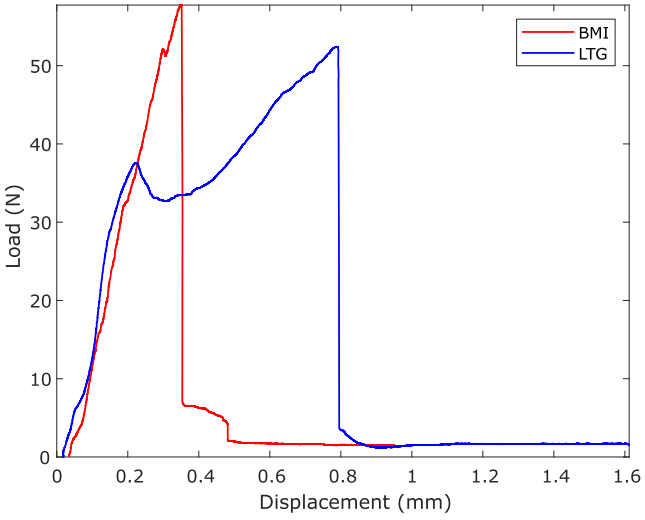

Fig. 17. Representative load–displacement curves for both BMI and LTG pins at a load mode-mixity ratio of 0.7. (For interpretation of the references to colour in this figure legend, the reader is referred to the web version of this article.)

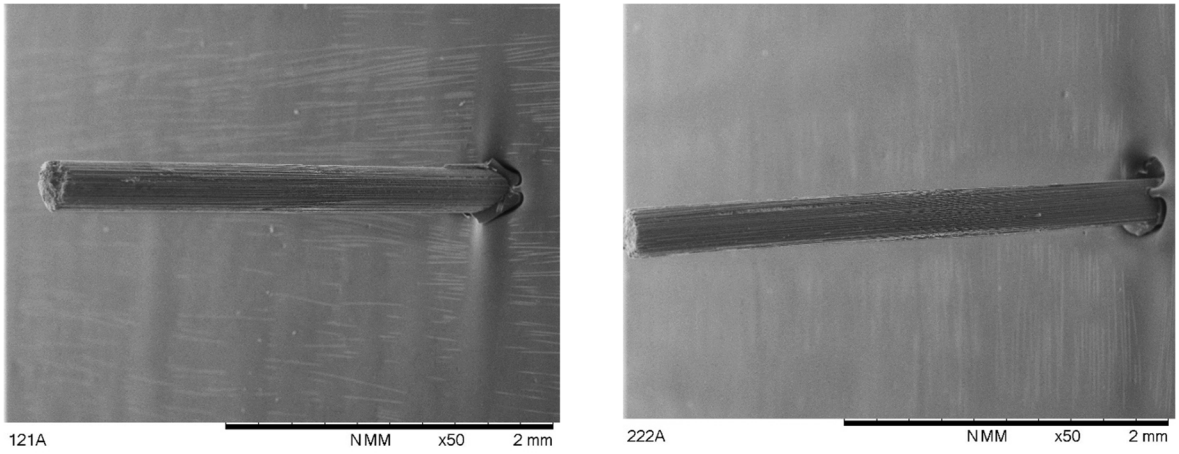

Fig. 16. SEM images of BMI (left) and LTG (right) Z-pins pulled out under primarily mode-I loading conditions.

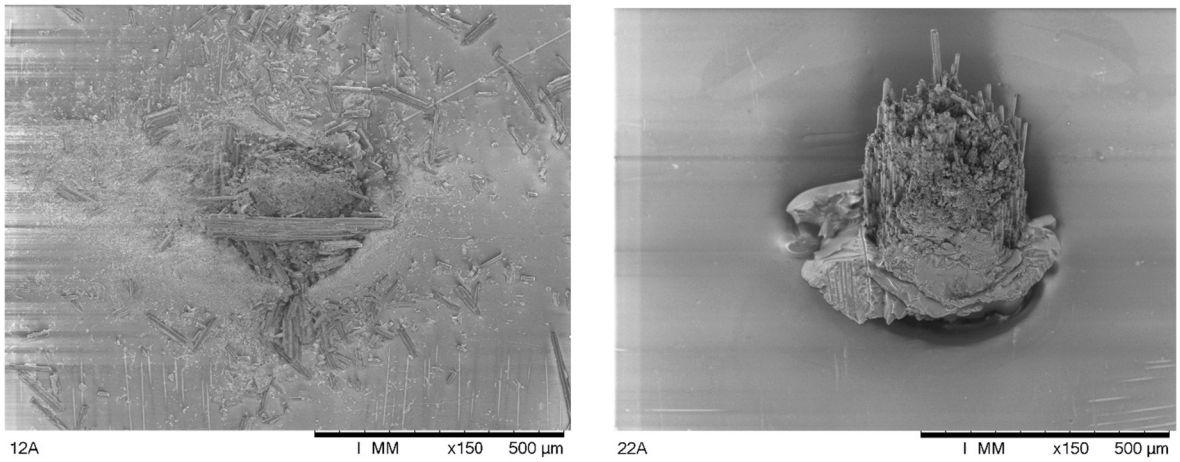

Fig. 18. SEM images of BMI (left) and LTG (right) Z-pins which ruptured at load mode-mixity ratio of 0.7.

allows the Z-pin to withstand much larger bending and shearing deformations compared to through-thickness reinforcement manufactured using brittle BMI. The large rotation of the Z-pin cross section enabled by the ductile matrix causes a re-orientation of the transverse load towards the Z-pin axis, which allows pull-out at mode-mixity values that approach 0.6, whereas BMI-based through-thickness reinforcement typically starts failing at a mode-mixity of 0.2. Hence, a Z-pin comprising a ductile matrix has an extended pull-out range and enhanced mixed-mode bridging performance compared to through-thickness reinforcement with entirely brittle constituents.

3. The adoption of the LTG ductile matrix in a Z-pin is also beneficial for mode I performance, as it causes higher interface friction during pull out.
4. The mode II interlaminar toughness of Z-pinned laminates is unaffected by the matrix constituent of the through-thickness reinforcement, since it is primarily controlled by the fracture toughness for tensile fibre failure of the Z-pin. This is confirmed by the fact that Z-pins with different matrix formulations but the same fibre type (*i.e.* T300 in this study) yield the same value of mode II interlaminar fracture toughness.

As a closing remark, it must be noted that the results presented here only involve single-pin delamination tests in a pre-cracked laminate. The effectiveness of the proposed ductile-matrix solution for arrays of Z-pins in laminates that experience progressive delamination is currently being investigated and it will be reported in a separate paper.

CRediT authorship contribution statement

E. Santana de Vega: Conceptualization, Methodology, Validation, Investigation, Data curation, Writing – original draft, Visualization. **G. Allegri:** Conceptualization, Methodology, Writing – review & editing, Supervision, Project administration, Resources, Funding acquisition. **B. Zhang:** Conceptualization, Methodology, Writing – review & editing, Supervision, Resources. **I. Hamerton:** Conceptualization, Writing – review & editing, Supervision, Resources. **S.R. Hallett:** Conceptualization, Writing – review & editing, Supervision, Project administration, Resources, Funding acquisition.

Declaration of Competing Interest

The authors declare that they have no known competing financial interests or personal relationships that could have appeared to influence the work reported in this paper.

Data availability

Data will be made available on request.

Acknowledgements

The authors wish to acknowledge the support of Rolls-Royce plc through the Composites University Technology Centre (UTC) at the University of Bristol and the EPSRC through the ACCIS Centre for Doctoral Training grant, no. EP/G036772/1.

References

[1] Mouritz AP, Bannister MK, Falzon PJ, Leong KH. Review of applications for advanced three-dimensional fibre textile composites. Compos Part A Appl Sci Manuf 1999;30:1445–61. https://doi.org/10.1016/S1359-835X(99)00034-2.
[2] Warrior NA, Rudd CD, Gardner SP. Experimental studies of embroidery for the local reinforcement of composites structures: 1. Stress concentrations. Compos Sci Technol 1999;59:2125–37. https://doi.org/10.1016/s0266-3538(99)00071-8.
[3] Dell'Anno G, Treiber JWG, Partridge IK. Manufacturing of composite parts reinforced through-thickness by tufting. Robot Comput Integr Manuf 2016;37:262–72. https://doi.org/10.1016/j.rcim.2015.04.004.
[4] Cartié DDR, Cox BN, Fleck NA. Mechanisms of crack bridging by composite and metallic rods. Compos Part A Appl Sci Manuf 2004;35:1325–36. https://doi.org/10.1016/j.compositesa.2004.03.006.
[5] Mouritz AP. Review of z-pinned laminates and sandwich composites. Compos Part A Appl Sci Manuf 2020;139:106128. https://doi.org/10.1016/j.compositesa.2020.106128.
[6] Mouritz AP. Review of z-pinned composite laminates. Compos Part A Appl Sci Manuf 2007;38:2383–97. https://doi.org/10.1016/j.compositesa.2007.08.016.
[7] Kostopoulos V, Sarantinos N, Tsantzalis S. Review of Through-the-Thickness Reinforced z-Pinned Composites. J Compos Sci 2020;4:31. https://doi.org/10.3390/jcs4010031.
[8] Partridge IK, Cartié DDR. Delamination resistant laminates by Z-Fiber® pinning: Part I manufacture and fracture performance. Compos Part A Appl Sci Manuf 2005;36:55–64. https://doi.org/10.1016/j.compositesa.2004.06.029.
[9] Cartié DDR, Troulis M, Partridge IK. Delamination of Z-pinned carbon fibre reinforced laminates. Compos Sci Technol 2006;66:855–61. https://doi.org/10.1016/j.compscitech.2004.12.018.
[10] Yasaee M, Lander JK, Allegri G, Hallett SR. Experimental characterisation of mixed mode traction-displacement relationships for a single carbon composite Z-pin. Compos Sci Technol 2014;94:123–31. https://doi.org/10.1016/j.compscitech.2014.02.001.
[11] Chang P, Mouritz AP, Cox BN. Properties and failure mechanisms of z-pinned laminates in monotonic and cyclic tension. Compos Part A Appl Sci Manuf 2006;37:1501–13. https://doi.org/10.1016/j.compositesa.2005.11.013.
[12] Pegorin F, Pingkarawat K, Daynes S, Mouritz AP. Influence of z-pin length on the delamination fracture toughness and fatigue resistance of pinned composites. Compos Part B Eng 2015;78:298–307. https://doi.org/10.1016/j.compositesb.2015.03.093.
[13] Pegorin F, Pingkarawat K, Mouritz AP. Comparative study of the mode I and mode II delamination fatigue properties of z-pinned aircraft composites. Mater Des 2015;65:139–46. https://doi.org/10.1016/j.matdes.2014.08.072.
[14] Warzok F, Allegri G, Gude M, Hallett SR. Experimental study of Z-pin fatigue; understanding of mode I and II coupon behaviour. Compos Part A Appl Sci Manuf 2019;127:105615. https://doi.org/10.1016/j.compositesa.2019.105615.

[15] Cui H, Mahadik Y, Hallett SR, Partridge IK, Allegri G, Ponnusami SA, et al. Coupon scale Z-pinned IM7/8552 delamination tests under dynamic loading. Compos Part A Appl Sci Manuf 2019;125:105565. 10.1016/j.compositesa.2019.105565.
[16] Cui H, Yasaee M, Kalwak G, Pellegrino A, Partridge IK, Hallett SR, et al. Bridging mechanisms of through-thickness reinforcement in dynamic mode I&II delamination. Compos Part A Appl Sci Manuf 2017;99:198–207. https://doi.org/10.1016/j.compositesa.2017.04.009.
[17] Son HG, Bin PY, Kweon JH, Choi JH. Fatigue behaviour of metal pin-reinforced composite single-lap joints in a hygrothermal environment. Compos Struct 2014;108:151–60. https://doi.org/10.1016/j.compstruct.2013.09.012.
[18] Heimbs S, Nogueira AC, Hombergsmeier E, May M, Wolfrum J. Failure behaviour of composite T-joints with novel metallic arrow-pin reinforcement. Compos Struct 2014;110:16–28. https://doi.org/10.1016/j.compstruct.2013.11.022.
[19] M'membe B, Yasaee M, Hallett SR, Partridge IK. Effective use of metallic Z-pins for composites' through-thickness reinforcement. Compos Sci Technol 2019;175:77–84.
[20] Allegri G, Yasaee M, Partridge IK, Hallett SR. A novel model of delamination bridging via Z-pins in composite laminates. Int J Solids Struct 2014;51:3314–32. https://doi.org/10.1016/j.ijsolstr.2014.05.017.
[21] Mouritz AP, Koh TM. Re-evaluation of mode i bridging traction modelling for z-pinned laminates based on experimental analysis. Compos Part B Eng 2014;56:797–807. https://doi.org/10.1016/j.compositesb.2013.09.016.
[22] Huntsman. Araldite ® LY 3508* / Aradur ® 22962* 2012:1–5.
[23] Huntsman. Araldite ® LY 556/ Hardener XB 3473 2007:1–5.
[24] Hamerton I, Iredale RJ. On the natural selection of high performance polymers 2021. 10.24820/ark.5550190.p011.517.
[25] Iredale RJ. Solvent-free, liquid processable bismaleimide-triazine resins. 2019.
[26] Zhang B, Allegri G, Yasaee M, Hallett SR. Micro-mechanical finite element analysis of Z-pins under mixed-mode loading. Compos Part A Appl Sci Manuf 2015;78:424–35. https://doi.org/10.1016/j.compositesa.2015.07.006.
[27] Sweeting RD, Thomson RS. The effect of thermal mismatch on Z-pinned laminated composite structures. Compos Struct 2004;66:189–95. https://doi.org/10.1016/j.compstruct.2004.04.037.
[28] Cartié DDR, Partridge IK. Effect of Z-Fibres on the delamination behaviour of carbon fibre / epoxy laminates. Sch Ind Manuf Sci 2000;PhD..
[29] M'membe B, Gannon S, Yasaee M, Hallett SR, Partridge IK. Mode II delamination resistance of composites reinforced with inclined Z-pins. Mater Des 2016;94:565–72.
[30] Cui H, Li Y, Koussios S, Zu L, Beukers A. Bridging micromechanisms of Z-pin in mixed mode delamination. Compos Struct 2011;93:2685–95. https://doi.org/10.1016/j.compstruct.2011.06.004.